

Imaging pulsar echoes at low frequencies

Olaf Wucknitz*

Max-Planck-Institut für Radioastronomie, Auf dem Hügel 69, 53121 Bonn, Germany,

E-mail: wucknitz@mpifr-bonn.mpg.de

Interstellar scattering is known to broaden distant objects spatially and temporally. The latter aspect is difficult to analyse, unless the signals carry their own time stamps. Pulsars are so kind to do us this favour. Typically the signature is a broadened image with little or no substructure and a similarly smooth exponential scattering tail in the temporal profile. The case of the pulsar B1508+55 is special: The profile shows additional components that are moving relative to the main pulse with time. We use low-frequency VLBI with LOFAR to test the hypothesis that these components are actually such scattering-induced echoes, by trying to detect the expected angular offset. Using international stations (plus the Kilpisjärvi Atmospheric Imaging Receiver Array 'KAIRA') and the phased-up core of the LOFAR array, we can do interferometry at high resolution in time and space.

This contribution presents a selection of results from an ongoing large-scale monitoring campaign. We can not only detect the offset, but even image a full string of echoes, and relate the positions with delays. What we find is apparently consistent with scattering by highly aligned components in a single screen at a distance of 120 pc. Further investigations will improve our understanding of the scattering process as basis of using the scattering-induced subimages as arms of a giant interstellar interferometer with insanely high resolution.

14th European VLBI Network Symposium & Users Meeting (EVN 2018)

8-11 October 2018

Granada, Spain

*Speaker.

1. The ghost of B1508+55

The pulsar B1508+55 has $S \sim 800$ mJy near 150 MHz, which makes it an easy target for LOFAR (van Haarlem et al., 2013). Monitoring revealed interesting features (Verbiest, priv. comm.): Donner found significant DM variations that were followed up by Osłowski, using monitoring with GLOW stations.¹ Variability of the trailing edge of the profile were found in these data and independently in a monitoring campaign by Serylak. Macquart and Bhat hypothesised that the ‘ghost’ component(s) are likely caused by interstellar scattering and are not intrinsic to the pulsar itself.

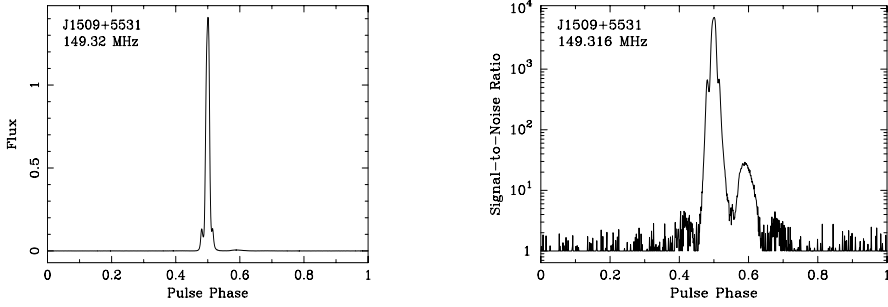


Figure 1: Profile of B1508+55 observed with LOFAR. The ghost near phase 0.6 (about 70 msec offset from the peak) becomes obvious on a logarithmic scale (right). Profiles kindly provided by Stefan Osłowski.

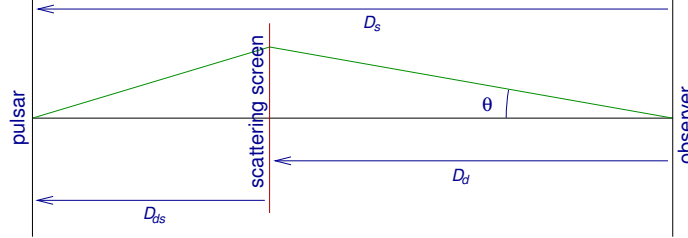


Figure 2: Scattering geometry with one subimage deflected by an apparent angle θ .

Extensive LOFAR monitoring confirmed the existence of the ghost components (see Fig. 1) and found that they are slowly approaching the main pulse with time. Scattered components are delayed, because their geometric path is slightly longer (see Fig. 2).

$$c\tau = \frac{1}{2}\theta^2 D \qquad D = \frac{D_s D_d}{D_{ds}}$$

D_s and D_d are the distances to the source and the deflector, respectively, and D_{ds} is the distance between deflector and source. For non-cosmological distances they are additive, $D_{ds} = D_s - D_d$.

For a first guess we assumed that the scattering screen is halfway between the pulsar and us, which corresponds to $D = D_s = 2.1$ kpc (Chatterjee et al., 2009). For a delay of 70 msec (see Fig. 1) the expected angle is $\theta = 0''.16$. This cannot be *resolved* with LOFAR at 150 MHz, but components separated by pulsar gating can be *localised* even better, provided the signal is strong enough.

¹The ‘German Long Wavelength Consortium’ (GLOW) coordinates local use of the German LOFAR stations.

2. Time-resolved VLBI with LOFAR

We have to correlate offline after recording baseband data because of the insufficient temporal resolution of the online correlator. This procedure is unusual for LOFAR, but not for VLBI. We started the observations in 2016 with the six German stations of the LOFAR array, which can be controlled and recorded centrally in Bonn and Jülich. Later we included all other international stations in France, Sweden, England, Poland (3), Ireland, the phased-up core and KAIRA in Northern Finland (McKay-Bukowski et al., 2015). The core is recorded centrally, but all other stations use their own recording equipment. Data are transferred electronically to Bonn.² The data rate is 3.1 Gbps per station, one hour with all stations amounts to ca. 20 TB of baseband data.

Data are correlated with an own software correlator. The main pulse is used as in-beam calibrator, so that positions and fluxes are relative to the unscattered pulsar itself. After correcting for possible amplitude and phase differences between the linear dipoles per station, we convert the signal to a circular polarisation basis using an approximated model of the instrument response.

The phases are calibrated with a station-based fringe-fitting algorithm that includes dispersive (ionospheric) and non-dispersive (clocks) delays, rates and differential Faraday rotation. Afterwards the amplitude bandpass is determined and corrected, and a second iteration of fringe-fitting is performed. The calibration solutions are then applied to the full set of time-resolved visibilities.

Data weights are derived from the autocorrelations, which automatically downweights visibilities affected by RFI, so that no flagging is needed. This is remarkable given the extremely strong

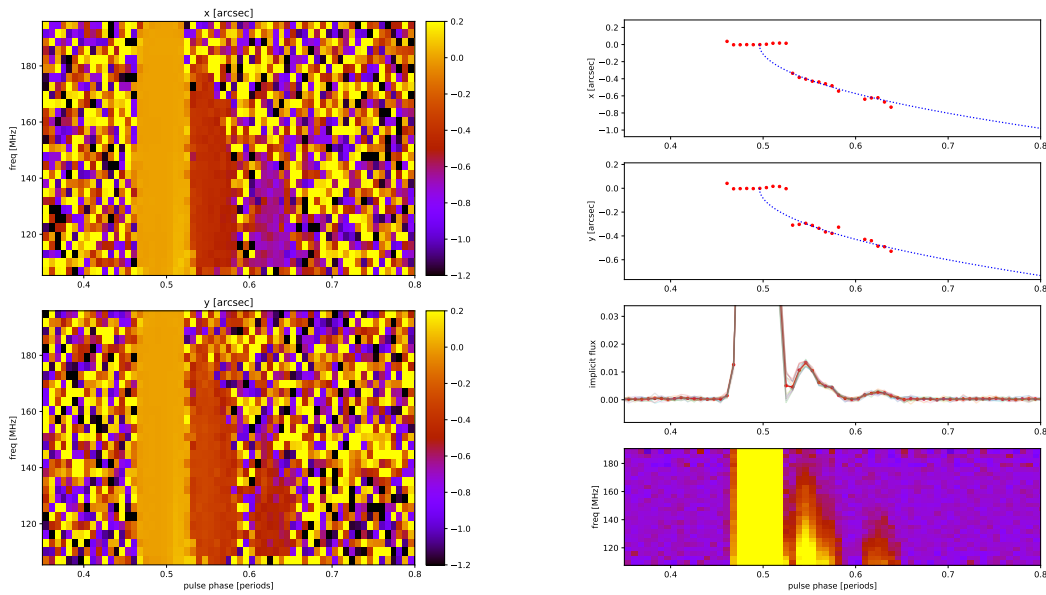


Figure 3: Left: Component position as function of pulse phase and frequency. Right: Component position (upper two panels); flux (third panel, combined and single baselines) as function of pulse phase; folded dynamic spectrum (bottom). The offset is consistent with the expected parabola. We also notice the steep spectrum of the echoes, which is consistent with scattering.

²For KAIRA this involves a physical transport of disks from the site to Tromsø. During winter and spring this can delay the data delivery significantly.

interference at certain frequencies and times. A disadvantage of this approach is that very bright pulses are downweighted slightly, whenever they reach a significant fraction of the system noise.

3. Gated analysis

After the phase and amplitude calibration we combine all baselines to measure the position and flux as function of pulse phase (proxy for delay) and frequency. Figure 3 shows clearly that the echoes are offset in position from the main pulse, which confirms the echo hypothesis. The effect is stronger than expected, which means the scattering medium must be closer to us. The positions are constant over the band so that we can combine all frequencies. The position relative to the main pulse follows the expected parabola from the relation $\tau \propto \theta^2$ quite well. From the slope of that parabola we get a first estimate of the distance to the scattering screen of approximately 124 pc.

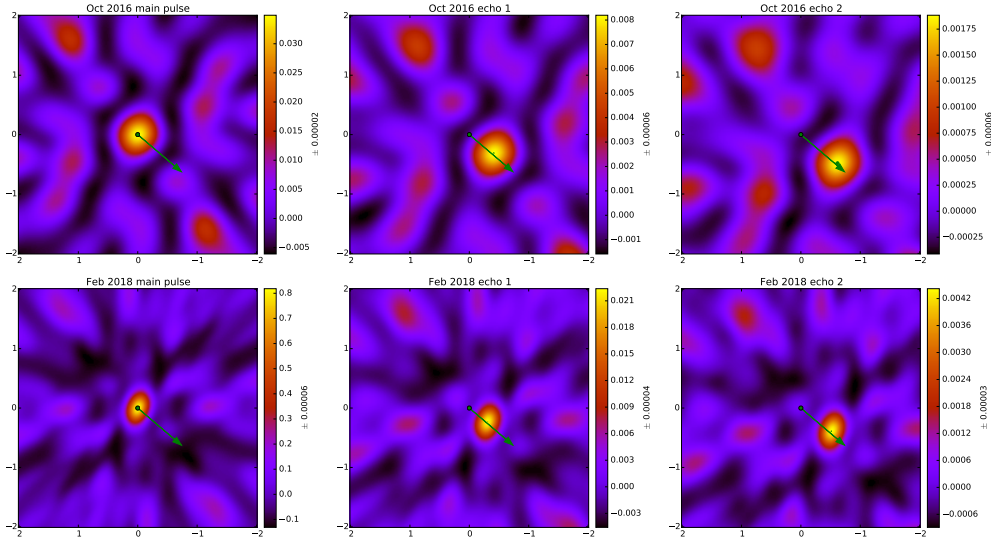


Figure 4: Gated dirty images of the main pulse (left) and the first two echoes (centre and right). The top panels are from October 2016 using GLOW only, the lower ones are with the international array. All features besides the main peak are sidelobes, the noise level is much lower. We notice the increased resolution with the full array. The arrow represents the pulsar proper motion of almost 100 mas/yr (Chatterjee et al., 2009). The alignment of the echo offsets with the proper motion seem to be accidental, even though some alignment is favoured by selection effects.

We continued observing the system more or less regularly, included KAIRA and later also the other international LOFAR stations and the core. Fig. 4 shows dirty images from early GLOW and later international data. We notice that the angular separation of the echoes from the main pulse decreases with time in a way that is consistent with the pulsar proper motion and fixed echo positions.

4. Deconvolution

The gated analysis presented so far is not optimal, because it is based on the invalid assumption that the intrinsic profile does not overlap with the echoes, and that delayed versions of the profile

do not overlap with each other. In order to solve this superposition problem, we are developing a method to combine the angular deconvolution (with the dirty beam) and the temporal deconvolution (with the pulse profile) into one algorithm. The current version is a generalisation of CLEAN. Standard CLEAN subtracts and collects components by position (and implicitly flux). Our delayed-profile-aware version of CLEAN uses the delay as additional explicit parameter and replaces the flux by a spectrum as implicit parameter. In this way the measured signal is decomposed into delayed and shifted version of the intrinsic pulse profile, each potentially with its own spectrum, because scattering is known to be strongly chromatic.

Figure 5 illustrates the deconvolution process. The method is not perfect, but it already separates the echoes from the wings of the intrinsic profile very well (blue and green curves in lower right panel). With simple gated imaging these components would be merged. The echo components fit the expected parabola (lower left panel for $D_d = 117$ pc) very well, even after more iterations. The deviations in the central area are at least partly due to inaccuracies of the deconvolution. This will be investigated further, because real deviations from the parabola are direct measurements of the delay happening in the scattering screen (in addition to the geometric delay) and would be evidence for larger-scale lensing effects.

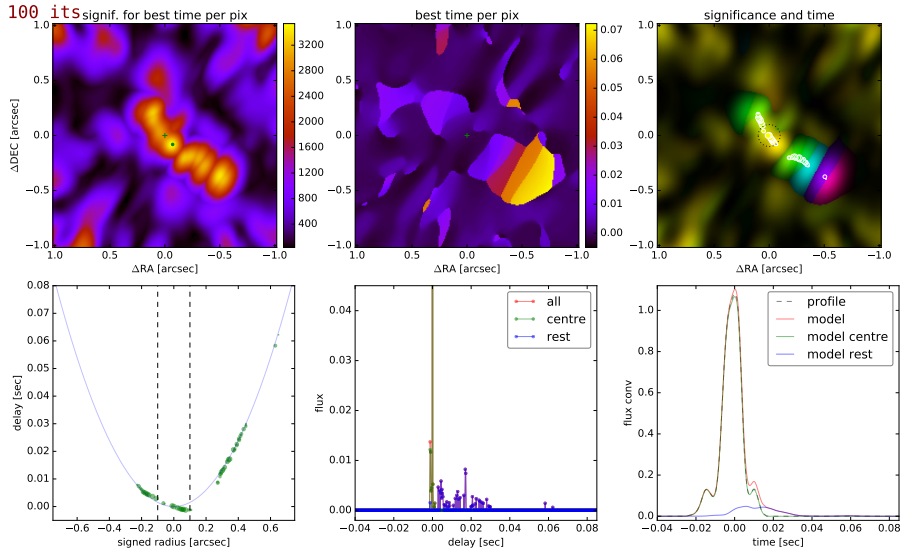


Figure 5: Intermediate results of our generalised CLEAN method after 100 iterations. Top: Residual map (significance as function of position, each for the optimum delay); optimum delay as function of position; the two combined (delay as colour, white circles show collected components). Bottom: Delay as function of signed radius (measured from upper left to bottom right) with expected parabola; components in delay space; the same convolved with the intrinsic profile and separated into central part and rest (echoes).

5. Discussion and outlook

Low-frequency VLBI proves the nature of the ghosts in B1508+55 as scattering-induced echoes and makes it possible to study the scattering process in unprecedented detail.

The fact that the string of echoes directly crosses the pulsar is at least consistent with a very anisotropic scattering that can deflect only in this direction. There are components on both sides,

which means that some must have crossed the line of sight in the past, to our knowledge without spectacular effects. This an important result in itself, because large-scale lensing would behave differently. It remains to be seen what crossings of the brighter components in the future will show.

With the current monitoring programme we will be able to follow the echo components in their evolution over time while the pulsar is moving behind them. Their behaviour provides important information about the density field that is causing the scattering. The alignment with the proper motion is still a puzzle, but it helps in accelerating the evolution in this system.

Possible physical models are under investigation, e.g. variants of ideas presented by Walker et al. (2017). There is indeed an A2 star 1.37 pc from the line of sight at a distance of (120 ± 8) pc, which is consistent with our estimate of the distance to the scattering screen. Intriguingly the offset is also aligned almost exactly with the line of echoes.

In the future we will also study other systems in the same way, e.g. B2217+47, in which Michilli et al. (2018) also find strong evidence for echoes.

Acknowledgments

Many thanks go to everybody who helped with the observations at all the stations, in particular (in alphabetic order) Leszek Błaskiewicz, Tobia Carozzi, Julian Donner, Jean-Mathias Grießmeier, Andreas Horneffer, Aris Karastergiou, Andrzej Krankowski, Jörn Künsemöller, Wojciech Lewandowski, Barbara Matyjasiak, Derek McKay, Natasha Porayko, Mariusz Pożoga, Hanna Rotkaehl, Tomasz Sidorowicz, Bartosz Śmierciak, Marian Soida, Caterina Tiburzi. Additional thanks go to Mark Walker and Artem Tuntsov for discussions about their model.

This work is based in part on results obtained with International LOFAR Telescope (ILT) equipment under project codes LC8_008, LC9_038, LC10_002. LOFAR is the Low Frequency Array designed and constructed by ASTRON. It has observing, data processing, and data storage facilities in several countries, that are owned by various parties (each with their own funding sources), and that are collectively operated by the ILT foundation under a joint scientific policy. The ILT resources have benefitted from the following recent major funding sources: CNRS-INSU, Observatoire de Paris and Université d'Orléans, France; BMBF, MIWF-NRW, MPG, Germany; Science Foundation Ireland (SFI), Department of Business, Enterprise and Innovation (DBEI), Ireland; NWO, The Netherlands; The Science and Technology Facilities Council, UK; Ministry of Science and Higher Education, Poland.

In particular we made use of data from the Effelsberg (DE601) station funded by the Max-Planck-Gesellschaft; the Unterweilenbach (DE602) station funded by the Max-Planck-Institut für Astrophysik, Garching; the Tautenburg (DE603) station funded by the State of Thuringia, supported by the European Union (EFRE) and the Federal Ministry of Education and Research (BMBF) Verbundforschung project D-LOFAR I (grant 05A08ST1); the Potsdam (DE604) station funded by the Leibniz-Institut für Astrophysik, Potsdam; the Jülich (DE605) station supported by the BMBF Verbundforschung project D-LOFAR I (grant 05A08LJ1); and the Norderstedt (DE609) station funded by the BMBF Verbundforschung project D-LOFAR II (grant 05A11LJ1). The observations of the German LOFAR stations were carried out in the stand-alone GLOW mode (German LOng-Wavelength array), which is technically operated and supported by the Max-Planck-Institut für Radioastronomie, the Forschungszentrum Jülich and Bielefeld University. We acknowledge support and operation of the GLOW network, computing and storage facilities by the FZ-Jülich, the MPIfR and Bielefeld University and financial support from BMBF D-LOFAR III (grant 05A14PBA), and by the states of Nordrhein-Westfalia and Hamburg.

References

- Chatterjee, S., Briskin, W. F., Vlemmings, W. H. T., et al. 2009, *ApJ*, 698, 250
 McKay-Bukowski, D., Vierinen, J., Virtanen, I. I., et al. 2015, *IEEE Trans. Geosci. Remote Sens.*, 53, 1440
 Michilli, D., Hessels, J. W. T., Donner, J. Y., et al. 2018, *MNRAS*, 476, 2704
 van Haarlem, M. P., Wise, M. W., Gunst, A. W., et al. 2013, *A&A*, 556, A2
 Walker, M. A., Tuntsov, A. V., Bignall, H., et al. 2017, *ApJ*, 843, 15